DMD Fast Forward. Published on December 31, 2020 as DOI: 10.1124/dmd.120.000283
This article has not been copyedited and formatted. The final version may differ from this version.

Title

In vivo gene expression profile of human intestinal epithelial cells: from the viewpoint of drug metabolism and pharmacokinetics

Authors and affiliations

Kazuo Takayama[1,2]

Kohei Ito[3]

Akiko Matsui[3]

Tomoki Yamashita[1]

Kentaro Kawakami[4]

Daisuke Hirayama[4]

Wataru Kishimoto[3*], wataru.kishimoto@boehringer-ingelheim.com

Hiroshi Nakase[4*], hiro_nakase@sapmed.ac.jp

Hiroyuki Mizuguchi[1,2,5,6*], mizuguch@phs.osaka-u.ac.jp

[1] Laboratory of Biochemistry and Molecular Biology, Graduate School of Pharmaceutical Sciences, Osaka University, Osaka 565-0871, Japan

[2] Laboratory of Hepatocyte Regulation, National Institutes of Biomedical Innovation, Health and Nutrition, Osaka 567-0085, Japan

[3] Department of Pharmacokinetics and Nonclinical Safety, Nippon Boehringer Ingelheim Co., Ltd., Kobe 650-0047, Japan

[4] Department of Gastroenterology and Hepatology, Sapporo Medical University School of Medicine, Sapporo 060-8543, Japan

[5] Global Center for Medical Engineering and Informatics, Osaka University, Osaka

565-0871, Japan

[6] Integrated Frontier Research for Medical Science Division, Institute for Open and Transdisciplinary Research Initiatives (OTRI), Osaka University, Osaka 565-0871, Japan

DMD Fast Forward. Published on December 31, 2020 as DOI: 10.1124/dmd.120.000283
This article has not been copyedited and formatted. The final version may differ from this version.

Running title

Gene expression profile of human intestinal epithelial cells

***Corresponding authors**

Dr. Wataru Kishimoto

Pharmacokinetic and Non-Clinical Safety department, Nippon Boehringer Ingelheim Co., Ltd., 6-7-5 Minatojima-Minamimachi, Chuo, Kobe, Hyogo 650-0047, Japan.

Phone: +81-78-306-4512, FAX: +81-78-306-1437

E-mail: wataru.kishimoto@boehringer-ingelheim.com

Dr. Hiroshi Nakase

Department of Gastroenterology and Hepatology, Sapporo Medical University School of Medicine, Sapporo 060-8543, Japan.

Phone: +81-11-611-2111, FAX: +81-11-613-1241

E-mail: hiro_nakase@sapmed.ac.jp

Dr. Hiroyuki Mizuguchi

Laboratory of Biochemistry and Molecular Biology, Graduate School of Pharmaceutical Sciences, Osaka University, 1-6 Yamadaoka, Suita, Osaka 565-0871, Japan.

Phone: +81-6-6879-8185, FAX: +81-6-6879-8187

E-mail: mizuguch@phs.osaka-u.ac.jp

Number of text pages: 37

DMD Fast Forward. Published on December 31, 2020 as DOI: 10.1124/dmd.120.000283
This article has not been copyedited and formatted. The final version may differ from this version.

Number of tables: 0

Figures: 10

References: 55

Number of words in the abstract: 246

Number of words in the introduction: 479

Number of words in the discussion: 656

Abbreviations

ADME	absorption, distribution, metabolism, and excretion
ASBT	ileal apical sodium/bile acid co-transporter
BCRP	breast cancer resistance protein
CES	carboxylesterase
CYBRD1	cytochrome b reductase 1
CYP	cytochrome P450
FXR	farnesoid X receptor
GATA4	GATA binding protein 4
GR	glucocorticoid receptor
HNF4A	hepatocyte nuclear factor 4 alpha
IBD	inflammatory bowel disease
iPS	induced pluripotent stem
LCA	lithocholic acid
LPH	lactase-phlorizin hydrolase
LRH1	liver receptor homolog-1
MCR	melanocortin receptor

DMD Fast Forward. Published on December 31, 2020 as DOI: 10.1124/dmd.120.000283
This article has not been copyedited and formatted. The final version may differ from this version.

MRP	multidrug resistance protein
OATP	organic anion transporting polypeptide
OST	organic solute transporter
PEPT1	peptide transporter 1
P-gp	P-glycoprotein
RIF	rifampicin
SULT	sulfotransferase
UGT	UDP-glucuronosyltransferase
VD3	1α,25-dihydroxyvitamin D3
VDR	vitamin D receptor

Key words : intestinal epithelial cells; biopsy; drug metabolizing enzymes; drug transporters; RNA-seq

DMD Fast Forward. Published on December 31, 2020 as DOI: 10.1124/dmd.120.000283
This article has not been copyedited and formatted. The final version may differ from this version.

Abstract

Orally administered drugs are absorbed and metabolized in the intestine. In order to accurately predict pharmacokinetics in the intestine, it is essential to understand the intestinal expression profiles of the genes related to drug absorption, distribution, metabolism, and excretion (ADME). However, in many previous studies, gene expression analysis in the intestine has been carried out using specimens from cancer patients. In this study, in order to obtain more accurate gene expression profiles, biopsy samples were collected under endoscopic observation from the non-inflammatory regions of 14 patients with inflammatory bowel disease and RNA-seq analysis was performed. Gene expression analysis of drug-metabolizing enzymes (*CYPs*), non-CYP enzymes, nuclear receptors, drug-conjugating enzymes (*UGTs* and *SULTs*), and apical and basolateral drug transporters was performed in biopsy samples from the duodenum, ileum, colon, and rectum. The proportions of the *CYPs* expressed in the ileum were 25% (*CYP3A4*), 19% (*CYP2C18*), and 14% (*CYP3A5*). *CYP3A4* and *CYP2C19* were highly expressed in the duodenum and ileum, but not in the colon and rectum. In the ileum, apical transporters such as *P-gp*, *PEPT1*, *BCRP*, *MRP2*, and *ASBT* were strongly expressed, and the expression levels of *P-gp* and *ASBT* in the ileum were higher than those in other regions. In the ileum, basolateral transporters such as *OSTα*, *OSTβ*, and *MRP3* were strongly expressed. We succeeded in obtaining gene expression profiles of ADME-related genes in human intestinal epithelial cells *in vivo*. We expect that this information would be useful for accurate prediction of the pharmacokinetics of oral drugs.

Significance Statement

DMD Fast Forward. Published on December 31, 2020 as DOI: 10.1124/dmd.120.000283
This article has not been copyedited and formatted. The final version may differ from this version.

To obtain gene expression profiles of ADME-related genes in human intestinal epithelial cells in vivo, biopsy samples were collected under endoscopic observation from the non-inflammatory regions of 14 patients with inflammatory bowel disease and RNA-seq analysis was performed. Gene expression profiles of drug-metabolizing enzymes (*CYPs*), non-CYP enzymes, nuclear receptors, drug-conjugating enzymes (*UGTs* and *SULTs*), and apical and basolateral drug transporters in biopsy samples from the duodenum, ileum, colon, and rectum were obtained in this study.

DMD Fast Forward. Published on December 31, 2020 as DOI: 10.1124/dmd.120.000283
This article has not been copyedited and formatted. The final version may differ from this version.

Introduction

Most orally administered drugs are absorbed and metabolized in the intestine. The intestinal tract plays an important role in the pharmacokinetics of orally administered drugs because drug-metabolizing enzymes, drug-conjugating enzymes, and drug transporters are highly expressed in the intestine. Therefore, to accurately predict the efficacy and side effects of orally administered drugs, it is necessary to understand the expression of drug absorption, distribution, metabolism, and excretion (ADME)-related genes in the intestinal tract. Although analysis of the intestinal expression of ADME-related genes has been performed using mice, rats, and pigs, it is known that there are species differences in the expression profiles of ADME-related genes (Martignoni et al., 2006). Therefore, it is essential to analyze the expression of ADME-related genes using human cells and specimens, not model animals. Previously, gene expression analysis was performed using cancer patients (Teubner et al., 2007). However, the gene expression profiles in cancer patients may differ from those in healthy individuals. In addition, some studies have analyzed intestinal epithelial cells that were isolated from a surgically removed intestinal tract that was transported outside the hospital [3, 4], but in these cases the phenotype of the intestinal epithelial cells could have changed before analysis. Therefore, there is a need for analysis using human specimens that are closer to physiological conditions. In this study, we collected intestinal biopsy samples from the non-inflammatory regions of patients with inflammatory bowel disease (IBD) because it is difficult to obtain intestinal biopsy samples from healthy donors.

Until now, expression analysis of ADME-related genes using human specimens has mostly been based on semi-quantitative PCR (Zhang et al., 1999), real-time PCR

DMD Fast Forward. Published on December 31, 2020 as DOI: 10.1124/dmd.120.000283
This article has not been copyedited and formatted. The final version may differ from this version.

(Hruz et al., 2006), and immunological analysis (Paine et al., 2006; Vaessen et al., 2017). Because ADME-related genes that were not intentionally selected may play an important role, it is important to perform not only an expression analysis of the intentionally selected genes but also a more unbiased comprehensive gene expression analysis. To the best of our knowledge, however, no studies have described the comprehensive gene expression profiles in each region of the human intestinal tract. RNA-seq is known to be an excellent method for comprehensive gene expression analysis. RNA-seq analysis not only enables detection of novel transcripts, but also allows for higher resolution analysis over a wider dynamic range. Therefore, we performed RNA-seq analysis using a HiSeq 4000 system to obtain a comprehensive gene expression profile with high accuracy and abundant information.

In this study, we first obtained biopsy samples of the duodenum, ileum, colon, and rectum from patients, and then performed RNA-seq analysis. Because the majority of the biopsy samples were composed of epithelial cells, the RNA-seq results are likely to reflect the gene expression profiles of intestinal epithelial cells. Because we were interested in the pharmacokinetics, we focused on the expression of drug-metabolizing enzymes (*cytochrome P450* (*CYPs*)), non-CYP enzymes, nuclear receptors, drug-conjugating enzymes (*UDP-glucuronosyltransferases* (*UGTs*) and *sulfotransferases* (*SULTs*)), and drug transporters. We believe that the data obtained in this study will be an important resource in pharmacokinetics.

DMD Fast Forward. Published on December 31, 2020 as DOI: 10.1124/dmd.120.000283
This article has not been copyedited and formatted. The final version may differ from this version.

Materials and Methods

Human intestinal biopsy samples

This study was approved by the institutional review board at Sapporo Medical University and Osaka University. We obtained written informed consent from all participants. This study was performed in accordance with the Declaration of Helsinki and the Human Ethical Guidelines of the Ministry of Health, Labour, and Welfare of Japan. Eligibility criteria were (1) a confirmed diagnosis of Crohn's disease or ulcerative colitis according to Japanese clinical guidelines (Matsuoka et al., 2018), (2) ≥20 years old with adequate organ function. Exclusion criteria was as follows; (1) history of cancer and (2) patients with venous thromboembolism requiring anticoagulants. Intestinal biopsy samples were collected using cold biopsy forceps from the small intestine (duodenum and ileum) or large intestine during upper gastrointestinal endoscopy, small intestine endoscopy, and lower gastrointestinal endoscopy. Intestinal biopsy samples were collected once from each region of the intestinal tract described above from each individual. Each intestinal biopsy sample was immediately placed into RNA later reagent (QIAGEN) and stored at -80°C. Note that some samples were obtained from patients treated with prednisolone or budesonide. Samples exposed to prednisolone or budesonide are marked with a *1 or *2, respectively (**Fig. 1E**).

RNA preparation and RNA-seq analysis

Total RNA from 23 fresh-frozen biopsies was isolated by QIAzol (QIAGEN) extraction after removal of RNA later reagent. The RNA samples were purified using an RNeasy Mini kit (QIAGEN). For evaluation of RNA quality, a BioAnalyzer (Agilent Technologies) and RNA 6000 nano chip (Agilent Technologies) were used and it was

DMD Fast Forward. Published on December 31, 2020 as DOI: 10.1124/dmd.120.000283
This article has not been copyedited and formatted. The final version may differ from this version.

confirmed that all RNA samples had an RNA integrity number (RIN) higher than 7. Library construction for RNA sequencing was performed using a TruSeq™ Stranded Total RNA Library Prep kit (Illumina).

For sequencing, a Hiseq 4000™ system (Illumina) was used to generate the FASTQ files. FastQC (http://www.bioinformatics.babraham.ac.uk/projects/fastqc), FASTX (http://hannonlab.cshl.edu/fastx_toolkit/index.html), and FastQ Screen (Wingett and Andrews, 2018) were utilized to check the quality of the FASTQ files. Single end reads from FASTQ files were mapped against the Genome Reference Consortium Human Build 38 using the STAR aligner (Dobin et al., 2013). The quantification and normalization (Trimmed mean of M-values (TMM (Robinson and Oshlack, 2010)) or Transcripts per million (TPM (Wagner et al., 2012))) were done by using Strand NGS 3.4 (Strand Life Sciences). The TMM/TPM normalization was performed on all sample sets, including *in vivo* human intestinal epithelial cells, human iPS cell-derived intestinal epithelial cells, and Caco-2 cells.

The data is available at Gene Expression Omnibus (GEO), and its accession number is GSE156453.

Caco-2 cell culture

Caco-2 cells were obtained from the Leibniz Institute DSMZ-German Collection of Microorganisms and Cell Cultures, Germany. Caco-2 cells were maintained at 37°C, 8% CO_2 and 95% relative humidity in a cell culture dish supplemented with DMEM + 3.7 g/L $NaHCO_3$ (Biochrom AG), MEM-NEAA (Thermo Fisher Scientific), L-Glutamine (Biochrom AG), penicillin-streptomycin (Thermo Fisher Scientific) and 10% FBS (Gibco, Themo Fisher Scientific). The passage number

DMD Fast Forward. Published on December 31, 2020 as DOI: 10.1124/dmd.120.000283
This article has not been copyedited and formatted. The final version may differ from this version.

of the Caco-2 cells was between 60 and 90. Total RNA was extracted and purified by using an RNeasy Mini kit (QIAGEN) according to manufacturer's standard protocol. RNA quality was evaluated in the same way as the biopsy samples using the BioAnalyzer (Agilent Technologies).

Human iPS cell culture

The human iPS cell line, YOW-iPS cell (Takayama et al., 2014), was maintained on a feeder layer of mitomycin C-treated MEF (mouse embryonic fibroblasts, Millipore) with ReproStem medium (ReproCELL) supplemented with 10 ng/ml fibroblast growth factor 2 (FGF2, KATAYAMA CHEMICAL INDUSTRIES).

Intestinal differentiation of human iPS cells

Intestinal differentiation of human iPS cells was performed according to our previous report (Takayama et al., 2019). Before the initiation of intestinal differentiation, human iPS cells were dissociated into clumps by using dispase (Roche) and plated onto the BD Matrigel Matrix Growth Factor Reduced (BD Biosciences)-coated apical chamber of BD Falcon cell culture inserts (6-well plate, 1.0 μm pore size, 1.6×10^6 pores/cm, PET Membrane). These cells were cultured in the MEF-conditioned medium for 2-3 days. For the definitive endoderm differentiation, human iPS cells were cultured for 4 days in RPMI1640 medium (Sigma-Aldrich) containing 100 ng/ml Activin A (R&D Systems), 1×GlutaMAX (Thermo Fisher Scientific), penicillin-streptomycin, and 1×B27 Supplement Minus Vitamin A (Thermo Fisher Scientific). During the definitive endoderm differentiation, the mesendoderm cells (day 2) were transduced with 3,000 vector particles (VP)/cell of FOXA2-expressing adenovirus (Ad) vector (Ad-FOXA2)

DMD Fast Forward. Published on December 31, 2020 as DOI: 10.1124/dmd.120.000283
This article has not been copyedited and formatted. The final version may differ from this version.

for 1.5 hr to promote definitive endoderm differentiation.

For the induction of intestinal progenitor cells, the definitive endoderm cells were cultured for 4 days in the intestinal differentiation medium [DMEM, high glucose (FUJIFILM Wako) containing 5 μM 6-bromoindirubin-3'-oxime (BIO; Calbiochem), 1×MEM Non-Essential Amino Acids Solution (Thermo Fisher Scientific), penicillin-streptomycin, 1×GlutaMAX, and 100 μM β-mercaptoethanol] supplemented with 10 μM N-[(3,5-difluorophenyl) acetyl]-L-alanyl-2-phenyl-1, 1-dimethylethyl ester-glycine (DAPT; Peptide Institute), and 10% Knockout Serum Replacement (Thermo Fisher Scientific).

For the induction of intestinal epithelial cell monolayers, the intestinal progenitor cells were cultured for 11 days in intestinal differentiation medium supplemented with 1 μM BIO and 2.5 μM DAPT, and then cultured for 15 days in the Wnt-3A-conditioned intestinal differentiation medium supplemented with 0.1 μM BIO, 1 μM DAPT, 250 ng/ml EGF, and 10 μM SB431542. During the intestinal differentiation, the intestinal progenitor cells (day 8) were transduced with 3,000 VP/cell of Ad-CDX2 (caudal-related homeobox transcription factor 2) for 1.5 hr to promote intestinal differentiation.

Statistical analysis

For hierarchical clustering/ heatmap generation and 3D PCA analysis human intestinal epithelial cells *in vivo*, TCC-GUI (Su et al., 2019) and GeneSpringGX software ver.14.9 (Agilent Technologies) were used, respectively. For clustering metric, Spearman's rank correlation coefficient value was used for assessing similarity among samples and the unweighted pair group method with arithmetic mean (UPGMA) was

DMD Fast Forward. Published on December 31, 2020 as DOI: 10.1124/dmd.120.000283
This article has not been copyedited and formatted. The final version may differ from this version.

used for creating a dendrogram. In **figures 3-8**, statistical analyses were performed using GraphPad Prism software.

DMD Fast Forward. Published on December 31, 2020 as DOI: 10.1124/dmd.120.000283
This article has not been copyedited and formatted. The final version may differ from this version.

Results

Acquisition of *in vivo* human intestinal epithelial cells

To obtain a gene expression profile of human intestinal epithelial cells *in vivo,* intestinal biopsy samples were collected under endoscopic observation from the non-inflammatory regions of 14 patients with inflammatory bowel disease (IBD). In this study, biopsy samples of the duodenum, ileum, colon, and rectum were collected. **Figure 1** presents images before and after collecting the biopsy sample from the duodenum: images of the inside of the duodenum (**Fig. 1A**), the collection of a biopsy sample using forceps (**Fig. 1B**), and a collected biopsy sample (**Fig. 1C**) are shown. Note that the intestinal biopsy samples were collected from endoscopically normal regions of the IBD patients. Biopsy samples of the duodenum, ileum, colon, and rectum were obtained from 4, 7, 10, and 2 patients, respectively (**Fig. 1D**). The gender, age, and race of patients who provided the biopsy samples are shown in **Figure 1E**. The RNA Integrity Number (RIN) and label of RNA collected from biopsy samples are also shown in **Figure 1E**. RNA-seq analysis was performed according to the procedure in **Figure S1A**. The equipment and analysis software used for the RNA-seq are shown in **Figure S1B**. The heat-map in **Figure 2A** and the PCA analysis of **Figure 2B** showed that the gene expression profiles of the duodenum, ileum, colon, and rectum biopsy samples could be divided into the respective regions. In addition, scatter and volcano plots are shown in **Figures S2-4** (**Fig. S2**: ileum vs duodenum; **Fig. S3**: ileum vs colon; **Fig. S4**: ileum vs rectum). These plots suggest that the difference in the gene expression levels between the ileum and duodenum is smaller than the difference in the gene expression levels between the ileum and rectum.

DMD Fast Forward. Published on December 31, 2020 as DOI: 10.1124/dmd.120.000283
This article has not been copyedited and formatted. The final version may differ from this version.

Expression analysis of CYPs in the intestinal tract

Previous human studies showed that intestinal CYP3A contributes significantly to the first-pass metabolism of several drugs, such as cyclosporine, midazolam, and verapamil (Kolars et al., 1991; Paine et al., 1996; von Richter et al., 2001). In this study, we examined the expression profile of CYPs in human intestinal epithelial cells *in vivo*. The proportions of the *CYPs* expressed in the ileum were 25% (*CYP3A4*), 19% (*CYP2C18*), 14% (*CYP3A5*), 10% (*CYP2J2*), 9% (*CYP27A1*), and 6% (*CYP4F12*) (**Fig. 3A**). In contrast, Paine *et al*. reported that *CYP3A* was the most abundant CYP (80%), followed by *CYP2C9* (15%), *CYP2C19* (2.9%), *CYP2J2* (1.4%), and *CYP2D6* (1%) (Paine et al., 2006). This difference might have been due to differences in the sample state, acquisition region, and analysis methods used. Although previous studies observed that intestinal CYP3A expression was the highest in the proximal region and then declined sharply toward the distal ileum (De Waziers et al., 1990; Paine et al., 1997; Zhang et al., 1999; Paine et al., 2006), in our experiments there were no differences in *CYP3A4* and *CYP3A5* expression levels between the duodenum and ileum (**Fig. 3B**). In addition, we observed few differences between *CYP3A4* and *CYP3A5* expression levels in the ileum, while Zhang *et al*. detected no CYP3A5 expression in human small intestine enterocytes (Zhang et al., 1999). As mentioned above, because the present study used an RNA-seq approach in small intestinal epithelial cells *in vivo*, we were able to obtain *CYP* expression profiles that were more detailed and comprehensive than those in previous reports.

Expression analysis of non-CYP enzymes in the intestinal tract

DMD Fast Forward. Published on December 31, 2020 as DOI: 10.1124/dmd.120.000283
This article has not been copyedited and formatted. The final version may differ from this version.

We next examined the expression profile of non-CYP enzymes in human intestinal epithelial cells *in vivo*. The proportions of the non-CYP enzymes expressed in the ileum were 20% (*AKR1B10*), 16% (*MAOA*), 14% (*CES2*), 14% (*ALDH1A1*), 8% (*CBR1*), and 7% (*ALDH18A1*) (**Fig. 4A**). CES belongs to the phase I drug-metabolizing enzymes. CES hydrolyzes a variety of drug esters, amides, carbamates, and similar structures. In the human small intestine, CES2, but not CES1, is predominantly expressed (Imai et al., 2006; Zhang et al., 2020). Teketani *et al*. have reported that there is a steep proximal-to-distal gradient of CES activity in the human small intestine (Taketani et al., 2007). In agreement with a previous report (Imai et al., 2006), we found that *CES2* accounted for the majority (94.6%) of CES expressed in the ileum in our subjects. We also found that *CES2* expression levels in the duodenum and ileum were higher than those in the colon and rectum (**Fig. 4B**).

Expression analysis of drug transporters in the intestinal tract

Several uptake transporters, including organic anion transporting polypeptide (OATP) family members, peptide transporter 1 (PEPT1; SLC15A1), and ileal apical sodium/bile acid co-transporter (ASBT; SLC10A2) are highly expressed at the apical membrane of small intestinal epithelial cells (Giacomini et al., 2010; Drożdzik et al., 2020). In addition, several efflux pumps, including breast cancer resistance protein (BCRP; ABCG2) and P-glycoprotein (P-gp; MDR1, ABCB1), are highly expressed at the apical membrane of small intestinal epithelial cells (Giacomini et al., 2010; Drożdzik et al., 2020). On the other hand, heteromeric organic solute transporter (OSTα–OSTβ) and multidrug resistance protein 3 (MRP3; ABCC3) are highly expressed at the basolateral membrane of small intestinal epithelial cells (Giacomini et

DMD Fast Forward. Published on December 31, 2020 as DOI: 10.1124/dmd.120.000283
This article has not been copyedited and formatted. The final version may differ from this version.

al., 2010). However, the gene expression profiles of these transporters have not been fully elucidated in human intestinal epithelial cells *in vivo*. In addition, there have been no detailed examinations of the expression profiles of these transporters specific to each region of the intestinal tract. Therefore, we also investigated the expression profiles of apical and basolateral transporters in human intestinal epithelial cells *in vivo*. The proportions of the apical transporters expressed in the ileum were 28% (*PEPT1*), 26% (*P-gp*), 22% (*BCRP*), 7% (*MRP2*), and 6% (*ASBT*) (**Fig. 5A, left**). Consistent with our data, Harwood et al. showed that gene expression levels of *PEPT1* in the human ileum were higher than those of other transporters (Harwood et al., 2019). As for the basolateral transporters, the proportions in the ileum were 41% (*OSTβ*), 30% (*OSTα*), 10% (*MRP3*), 9% (*MRP1*), and 7% (*MRP5*) (**Fig. 5A, right**). The gene expression levels of *P-gp*, *PEPT1*, *BCRP*, and *ASBT* in the ileum were significantly higher than those in other regions (**Fig. 5B**). Hruz *et al*. analyzed human *ASBT* mRNA expression along the intestinal tract in biopsies of 14 control subjects and found that *ASBT* expression was higher in the ileum than in other intestinal regions (Hruz et al., 2006). This result was consistent with our findings. In addition, we found that *PEPT1* expression levels were approximately 37 times higher than *PEPT2* expression levels in the ileum (data not shown).

Expression analysis of nuclear receptors in the intestinal tract

CYP3A4 expression in the human intestinal tract can be induced by various drugs, such as rifampicin (RIF) and 1α,25-dihydroxyvitamin D3 (VD3) (Theodoropoulos et al., 2003; van de Kerkhof et al., 2008). Nuclear receptors, such as vitamin D receptor (VDR) and pregnane X receptor (PXR), mediate the CYP3A4

DMD Fast Forward. Published on December 31, 2020 as DOI: 10.1124/dmd.120.000283
This article has not been copyedited and formatted. The final version may differ from this version.

induction. It is also known that VDR functions as a receptor for the secondary bile acid lithocholic acid (LCA), which is hepatotoxic and a potential enteric carcinogen (Makishima et al., 2002). Farnesoid X receptor (FXR), which is known as a nuclear receptor for bile acids, induces genes involved in enteroprotection and inhibits bacterial overgrowth and mucosal injury in the ileum (Inagaki et al., 2006). However, the gene expression profiles of nuclear receptors have not been sufficiently examined. Therefore, we next investigated the expression profiles of nuclear receptors in human intestinal epithelial cells *in vivo*. The proportions of the nuclear receptors expressed in the ileum were 17% (*NR3C2*), 14% (*HNF4A*), 14% (*VDR*), 13% (*NR5A2*), and 8% (*NR1D2*) (**Fig. 6A**). The *RXRα*, *LXR*, *CAR*, and *SHP* expression levels in the ileum were low. The gene expression levels of *FXR* in the ileum were significantly higher than those in other regions (**Fig. 6B**). In addition, the gene expression levels of *GR* and *PXR* in the duodenum and ileum were higher than those in the colon and rectum (**Fig. 6B**). On the other hand, *VDR* was highly expressed in all regions (**Fig. 6B**). These results suggest that CYP3A4 induction potency and bile acid metabolism might show different functional levels depending on the region of the intestinal tract.

Expression analysis of UGTs in the intestinal tract

It has been reported that intestinal glucuronidation metabolism may have a greater impact on oral bioavailability than hepatic glucuronidation metabolism in humans (Mizuma, 2009). It is also known that *UGT1A8* and *UGT1A10* mRNA expressions could be detected in both the small intestine and colon, but not in the liver (Cheng et al., 1999). Accordingly, we also investigated the expression profile of UGTs in human intestinal epithelial cells *in vivo*. The proportions of the UGTs expressed in the

DMD Fast Forward. Published on December 31, 2020 as DOI: 10.1124/dmd.120.000283
This article has not been copyedited and formatted. The final version may differ from this version.

ileum were 21% (*UGT8*), 18% (*UGT1A10*), 14% (*UGT2B7*), 12% (*UGT2A3*), and 9% (*UGT1A1*) (**Fig. 7A**). We found that the levels of intestinal *UGT2A3*, *UGT1A8*, *UGT1A1*, and *UGT2B7* expression were highest in the proximal region, and then gradually declined toward the distal region (**Fig. 7B**). Consistently, Fritz et al. showed that the levels of *UGT1A* and *UGT2B7* expression were highest in the proximal region, and then gradually declined toward the distal region (Fritz et al., 2019). Strassburg *et al*. reported that *UGT1A1*, *UGT1A3*, *UGT1A4*, *UGT1A6*, *UGT1A10*, *UGT2B4*, *UGT2B7*, and *UGT2B15* mRNA could be detected, while *UGT1A5*, *UGT1A7*, *UGT1A8*, *UGT1A9*, and *UGT2B10* mRNA could not be detected in the small intestine (Strassburg et al., 2000). In their study, macroscopically and histologically normal intestinal tissue was obtained from 18 German patients. They collected large intestinal pieces (approximately 200 mg), while we collected small intestinal pieces (approximately 5 mg × 3 pieces). Therefore, the cell population composing the collected intestinal biopsy samples might have differed between the study of Strassburg *et al.* and our present study.

Expression analysis of SULTs in the intestinal tract

Soluble SULTs play an important role in the elimination of xenobiotics. SULT1A1, SULT1A3 and SULT1B1 have been found in all parts of the intestine (Teubner et al., 2007). In addition, SULT1E1 and SULT2A1 have been detected in the ileum (Teubner et al., 2007). However, the intestinal tissue samples in those experiments were obtained only from Caucasian patients with tumor (Teubner et al., 2007). In the present study, we examined the expression profile of SULTs in human intestinal epithelial cells which were obtained from patients without tumors. In agreement with the aforementioned study (Teubner et al., 2007), we found that

DMD Fast Forward. Published on December 31, 2020 as DOI: 10.1124/dmd.120.000283
This article has not been copyedited and formatted. The final version may differ from this version.

SULT2A1, *SULT1B1*, *SULT1A2*, *SULT1A1*, and *SULT1E1* were highly expressed in the ileum (**Fig. 8A**). Consistently, Zhang et al. reported that the SULT1A1 and SULT2A1 were highly expressed in the ileum (Zhang et al., 2020). We also found that the gene expression levels of *SULT1A1*, *SULT1A3* and *SULT1B1* in the colon were lower than those in other intestinal regions (**Fig. 8B**). It is known that there are large species differences in the expression profile of SULTs. Lin *et al*. reported that SULT1A1 was not expressed in pig small intestine (Lin et al., 2004). Meinl *et al*. reported that SULTs were not expressed in rat small intestine (Meinl et al., 2009). Therefore, it is essential to use a human cell model when evaluating SULT-mediated drug conjugation.

Identification of duodenum-, ileum-, colon-, and rectum-specific markers

Many intestinal region-specific markers have been reported so far. For example, GATA binding protein 4 (GATA4) is expressed in the proximal small intestine (Bosse et al., 2006). It is also known that duodenal cytochrome b reductase 1 (CYBRD1) is expressed only in the duodenum (McKie et al., 2001), lactase-phlorizin hydrolase (LPH) is mainly expressed in the jejunum (Krasinski et al., 1997), and apical ASBT is mainly expressed in the ileum (Shneider, 2001). We tried to find new intestinal region-specific markers by analyzing the RNA-seq results obtained in this study. The genes shown in **Figure 9** were suggested to be duodenum-, ileum-, colon-, and rectum-specific markers. However, before these genes can be used as duodenum-, ileum-, colon-, and rectum-specific markers, their expression must be analyzed by western blotting analysis or immunostaining analysis.

Next, therefore, we examined the expression profile of miRNAs in human intestinal epithelial cells *in vivo*. The proportions of the miRNAs expressed in the ileum

DMD Fast Forward. Published on December 31, 2020 as DOI: 10.1124/dmd.120.000283
This article has not been copyedited and formatted. The final version may differ from this version.

were 20% (*miR1244-2*), 18% (*miR621*), 16% (*miR1244-3*), 11% (*miR194-1*), and 7% (*miR3936*) (**Fig. S5**).

Expression analysis of human iPS cell-derived intestinal epithelial cells and Caco-2 cells

Recently, we succeeded in generating intestinal epithelial cells from human induced pluripotent stem (iPS) cells (Ozawa et al., 2015; Negoro et al., 2016; Negoro et al., 2018; Takayama et al., 2019). In the present study, therefore, we also compared the global gene expression profiles between *in vivo* intestinal epithelial cells and human iPS cell-derived intestinal epithelial cells. In addition, the global gene expression profile of Caco-2 cells was analyzed, because Caco-2 cells are a widely used cell model of intestinal drug metabolism and absorption. PCA analysis showed that the gene expression profiles of human iPS cell-derived intestinal epithelial cells and Caco-2 cells were very different from those of human intestinal epithelial cells *in vivo* (**Fig. 10**). The gene expression levels of some CYPs and transporters in human iPS cell-derived intestinal epithelial cells were significantly lower than those in human small intestine *in vivo*. In order to produce human iPS cell-derived intestinal epithelial cells having properties similar to human intestinal epithelial cells *in vivo*, it is necessary to improve the intestinal differentiation method.

DMD Fast Forward. Published on December 31, 2020 as DOI: 10.1124/dmd.120.000283
This article has not been copyedited and formatted. The final version may differ from this version.

Discussion

In this study, to obtain gene expression profiles in human intestinal epithelial cells *in vivo*, biopsy samples were collected and RNA-seq analysis was performed. The gene expression profiles of drug-metabolizing enzymes (CYPs), non-CYP enzymes, nuclear receptors, drug-conjugating enzymes (UGTs and SULTs), and drug transporters in biopsy samples from the duodenum, ileum, colon, and rectum were elucidated in this study.

We consider that the data obtained herein would be more reflective of physiological conditions than the data obtained from intestinal epithelial cells isolated from a surgically removed intestinal tract that was transported outside the hospital (Ho et al., 2017; Li et al., 2018). Since the human intestinal biopsies were obtained from non-cancer patients in this study, the gene expression profiles in endoscopically normal intestinal epithelial cells could be analyzed. Moreover, in this manner we were able to obtain gene expression profiles in intestinal epithelial cells that were not exposed to anticancer drugs. However, because the patients participating in this study suffered from IBD, their expression profiles of genes related to inflammation may have differed from those in healthy individuals. Note that some patients are treated with steroids, which might affect gene expression levels of drug-metabolizing enzymes. It may be possible to discover the cause of IBD by comparing the acquired data with the gene expression profile of healthy individuals.

Because the biopsy samples obtained in this study were 5 mg per piece, they did not contain much intestinal gland or muscular mucosa, and most of the constituent cells were intestinal epithelial cells. However, the proportion of intestinal epithelial cells in the obtained biopsy samples was not measured. To perform a more rigorous analysis

of gene expression profiles in intestinal epithelial cells, it will be necessary to perform gene expression analysis in a cell population in which the positive rate of intestinal epithelial cell markers is almost 100%. Therefore, in the future, we would like to acquire gene expression profiles in specific cell populations by performing cell sorting and single cell analysis.

In this study, we performed only RNA-seq analysis; we did not evaluate the protein expression level or activity of ADME-related genes. From the viewpoint of pharmacokinetics, it is important to evaluate the activity of ADME-related genes using each specific substrate. It is reported that the mRNA expression levels of ADME-related genes do not correlate with protein expression levels (Drozdzik et al., 2019; Couto et al., 2020). However, it was difficult to measure the activities of ADME-related genes on a sufficient scale and within an adequate time period using only the small amounts of intestinal biopsy samples obtained in this study. In the future, it is expected that various pharmacokinetic studies could be performed by establishing an amplifiable intestinal organoid from the obtained biopsy sample. The above studies can be sufficiently realized because there have been many reports on the establishment of small intestinal and large intestinal organoids (Sato et al., 2011; Fujii et al., 2018).

Because it is difficult to collect biopsy samples from the jejunum during upper gastrointestinal endoscopy, small intestine endoscopy, and lower gastrointestinal endoscopy, gene expression analysis in the jejunum was not performed in this study. However, it would be very useful if we could obtain the gene expression profiles of ADME-related genes in the jejunum in the future. We consider that it is necessary to carry out more accurate statistical analysis by obtaining samples of not only jejunum but also other parts from many patients.

DMD Fast Forward. Published on December 31, 2020 as DOI: 10.1124/dmd.120.000283
This article has not been copyedited and formatted. The final version may differ from this version.

We obtained a comprehensive gene expression profile of ADME-related genes in intestinal epithelial cells. In many cases published before, only the expression of specific ADME-related genes was examined. We expect that the comprehensive gene expression data obtained in this study will be a useful resource for future analyses, because it contains the expression profiles of all genes in normal human intestinal epithelial cells. In this study, RNA-seq data was analyzed from a pharmacokinetic point of view, but analysis from other points of view would also be significant.

Acknowledgments

We thank Ms. Junko Tanba, Mr. Hideyuki Koide, Ms. Yasuko Hagihara, Ms. Natsumi Mimura, and Ms. Ayaka Sakamoto for their excellent technical support. We are also grateful to Dr. Christian Schultheis and Marlene Sakowski (Boehringer Ingelheim Pharma GmbH & Co. KG) for the cDNA library preparation and sequencing, to Dr. Ramona Schmid (Boehringer Ingelheim Pharma GmbH & Co. KG) and Dr. Janine Roy (Staburo GmbH) for bioinformatics support including primary processing of the data and QC, and to Ms. Naoko Ohtsu for Caco-2 cell RNA preparation.

Authorship Contributions

Participated in research design: Takayama K., Kishimoto W., Nakase H., Mizuguchi H.

Conducted experiments: Ito K., Matsui A., Kawakami K., Hirayama D.

Contributed new reagents or analytic tools: Kawakami K., Hirayama D.

Performed data analysis: Ito K., Matsui A., Takayama K., Yamashita T.

Wrote or contributed to the writing of the manuscript: Takayama K., Kishimoto W., Nakase H., Mizuguchi H.

DMD Fast Forward. Published on December 31, 2020 as DOI: 10.1124/dmd.120.000283
This article has not been copyedited and formatted. The final version may differ from this version.

DMD Fast Forward. Published on December 31, 2020 as DOI: 10.1124/dmd.120.000283
This article has not been copyedited and formatted. The final version may differ from this version.

References

Bosse T, Piaseckyj CM, Burghard E, Fialkovich JJ, Rajagopal S, Pu WT, and Krasinski SD (2006) Gata4 is essential for the maintenance of jejunal-ileal identities in the adult mouse small intestine. *Molecular and cellular biology* **26:**9060-9070.

Cheng Z, Radominska-Pandya A, and Tephly TR (1999) Studies on the substrate specificity of human intestinal UDP-glucuronosyltransferases 1A8 and 1A10. *Drug Metabolism and Disposition* **27:**1165-1170.

Couto N, Al-Majdoub ZM, Gibson S, Davies PJ, Achour B, Harwood MD, Carlson G, Barber J, Rostami-Hodjegan A, and Warhurst G (2020) Quantitative proteomics of clinically relevant drug-metabolizing enzymes and drug transporters and their intercorrelations in the human small intestine. *Drug Metabolism and Disposition* **48:**245-254.

De Waziers I, Cugnenc P, Yang C, Leroux J, and Beaune P (1990) Cytochrome P 450 isoenzymes, epoxide hydrolase and glutathione transferases in rat and human hepatic and extrahepatic tissues. *Journal of Pharmacology and Experimental Therapeutics* **253:**387-394.

Dobin A, Davis CA, Schlesinger F, Drenkow J, Zaleski C, Jha S, Batut P, Chaisson M, and Gingeras TR (2013) STAR: ultrafast universal RNA-seq aligner. *Bioinformatics* **29:**15-21.

Drozdzik M, Busch D, Lapczuk J, Müller J, Ostrowski M, Kurzawski M, and Oswald S (2019) Protein abundance of clinically relevant drug transporters in the human liver and intestine: a comparative analysis in paired tissue specimens. *Clinical Pharmacology & Therapeutics* **105:**1204-1212.

Droździk M, Oswald S, and Droździk A (2020) Extrahepatic Drug Transporters in Liver Failure: Focus on Kidney and Gastrointestinal Tract. *International Journal of Molecular Sciences* **21**:5737.

Fritz A, Busch D, Lapczuk J, Ostrowski M, Drozdzik M, and Oswald S (2019) Expression of clinically relevant drug - metabolizing enzymes along the human intestine and their correlation to drug transporters and nuclear receptors: An intra - subject analysis. *Basic & clinical pharmacology & toxicology* **124**:245-255.

Fujii M, Matano M, Toshimitsu K, Takano A, Mikami Y, Nishikori S, Sugimoto S, and Sato T (2018) Human intestinal organoids maintain self-renewal capacity and cellular diversity in niche-inspired culture condition. *Cell stem cell* **23**:787-793. e786.

Giacomini KM, Huang S-M, Tweedie DJ, Benet LZ, Brouwer KL, Chu X, Dahlin A, Evers R, Fischer V, and Hillgren KM (2010) Membrane transporters in drug development. *Nature reviews Drug discovery* **9**:215.

Harwood MD, Zhang M, Pathak SM, and Neuhoff S (2019) The regional-specific relative and absolute expression of gut transporters in adult caucasians: a meta-analysis. *Drug Metabolism and Disposition* **47**:854-864.

Ho M-CD, Ring N, Amaral K, Doshi U, and Li AP (2017) Human enterocytes as an in vitro model for the evaluation of intestinal drug metabolism: characterization of drug-metabolizing enzyme activities of cryopreserved human enterocytes from twenty-four donors. *Drug Metabolism and Disposition* **45**:686-691.

Hruz P, Zimmermann C, Gutmann H, Degen L, Beuers U, Terracciano L, Drewe J, and Beglinger C (2006) Adaptive regulation of the ileal apical sodium dependent bile acid transporter (ASBT) in patients with obstructive cholestasis. *Gut* **55**:395-402.

Imai T, Taketani M, Shii M, Hosokawa M, and Chiba K (2006) Substrate specificity of

carboxylesterase isozymes and their contribution to hydrolase activity in human liver and small intestine. *Drug metabolism and disposition* **34:**1734-1741.

Inagaki T, Moschetta A, Lee Y-K, Peng L, Zhao G, Downes M, Ruth TY, Shelton JM, Richardson JA, and Repa JJ (2006) Regulation of antibacterial defense in the small intestine by the nuclear bile acid receptor. *Proceedings of the National Academy of Sciences* **103:**3920-3925.

Kolars JC, Watkins P, Merion RM, and Awni W (1991) First-pass metabolism of cyclosporin by the gut. *The Lancet* **338:**1488-1490.

Krasinski SD, Upchurch BH, Irons SJ, June RM, Mishra K, Grand RJ, and Verhave M (1997) Rat lactase-phlorizin hydrolase/human growth hormone transgene is expressed on small intestinal villi in transgenic mice. *Gastroenterology* **113:**844-855.

Li AP, Alam N, Amaral K, Ho M-CD, Loretz C, Mitchell W, and Yang Q (2018) Cryopreserved Human Intestinal Mucosal Epithelium: A Novel In Vitro Experimental System for the Evaluation of Enteric Drug Metabolism, Cytochrome P450 Induction, and Enterotoxicity. *Drug Metabolism and Disposition* **46:**1562-1571.

Lin Z, Lou Y, and Squires JE (2004) Molecular cloning and functional analysis of porcine SULT1A1 gene and its variant: a single mutation SULT1A1 causes a significant decrease in sulfation activity. *Mammalian genome* **15:**218-226.

Makishima M, Lu TT, Xie W, Whitfield GK, Domoto H, Evans RM, Haussler MR, and Mangelsdorf DJ (2002) Vitamin D receptor as an intestinal bile acid sensor. *Science* **296:**1313-1316.

Martignoni M, Groothuis GM, and de Kanter R (2006) Species differences between mouse, rat, dog, monkey and human CYP-mediated drug metabolism, inhibition and induction. *Expert opinion on drug metabolism & toxicology* **2:**875-894.

Matsuoka K, Kobayashi T, Ueno F, Matsui T, Hirai F, Inoue N, Kato J, Kobayashi K, Kobayashi K, and Koganei K (2018) Evidence-based clinical practice guidelines for inflammatory bowel disease. *Journal of gastroenterology* **53:**305-353.

McKie AT, Barrow D, Latunde-Dada GO, Rolfs A, Sager G, Mudaly E, Mudaly M, Richardson C, Barlow D, and Bomford A (2001) An iron-regulated ferric reductase associated with the absorption of dietary iron. *Science* **291:**1755-1759.

Meinl W, Sczesny S, Brigelius-Flohe R, Blaut M, and Glatt H (2009) Impact of gut microbiota on intestinal and hepatic levels of phase 2 xenobiotic-metabolizing enzymes in the rat. *Drug Metabolism and Disposition* **37:**1179-1186.

Mizuma T (2009) Intestinal glucuronidation metabolism may have a greater impact on oral bioavailability than hepatic glucuronidation metabolism in humans: a study with raloxifene, substrate for UGT1A1, 1A8, 1A9, and 1A10. *International journal of pharmaceutics* **378:**140-141.

Negoro R, Takayama K, Kawai K, Harada K, Sakurai F, Hirata K, and Mizuguchi H (2018) Efficient Generation of Small Intestinal Epithelial-like Cells from Human iPSCs for Drug Absorption and Metabolism Studies. *Stem cell reports* **11:**1539-1550.

Negoro R, Takayama K, Nagamoto Y, Sakurai F, Tachibana M, and Mizuguchi H (2016) Modeling of drug-mediated CYP3A4 induction by using human iPS cell-derived enterocyte-like cells. *Biochemical and biophysical research communications* **472:**631-636.

Ozawa T, Takayama K, Okamoto R, Negoro R, Sakurai F, Tachibana M, Kawabata K, and Mizuguchi H (2015) Generation of enterocyte-like cells from human induced pluripotent stem cells for drug absorption and metabolism studies in human small intestine. *Scientific reports* **5:**16479.

Paine MF, Hart HL, Ludington SS, Haining RL, Rettie AE, and Zeldin DC (2006) The human intestinal cytochrome P450 "pie". *Drug Metabolism and Disposition* **34:**880-886.

Paine MF, Khalighi M, Fisher JM, Shen DD, Kunze KL, Marsh CL, Perkins JD, and Thummel KE (1997) Characterization of interintestinal and intraintestinal variations in human CYP3A-dependent metabolism. *Journal of Pharmacology and Experimental Therapeutics* **283:**1552-1562.

Paine MF, Shen DD, Kunze KL, Perkins JD, Marsh CL, McVicar JP, Barr DM, Gillies BS, and Thummel KE (1996) First - pass metabolism of midazolam by the human intestine. *Clinical Pharmacology & Therapeutics* **60:**14-24.

Robinson MD and Oshlack A (2010) A scaling normalization method for differential expression analysis of RNA-seq data. *Genome biology* **11:**1-9.

Sato T, Stange DE, Ferrante M, Vries RG, Van Es JH, Van Den Brink S, Van Houdt WJ, Pronk A, Van Gorp J, and Siersema PD (2011) Long-term expansion of epithelial organoids from human colon, adenoma, adenocarcinoma, and Barrett's epithelium. *Gastroenterology* **141:**1762-1772.

Shneider BL (2001) Intestinal bile acid transport: biology, physiology, and pathophysiology. *Journal of pediatric gastroenterology and nutrition* **32:**407-417.

Strassburg CP, Kneip S, Topp J, Obermayer-Straub P, Barut A, Tukey RH, and Manns MP (2000) Polymorphic gene regulation and interindividual variation of UDP-glucuronosyltransferase activity in human small intestine. *Journal of Biological Chemistry* **275:**36164-36171.

Su W, Sun J, Shimizu K, and Kadota K (2019) TCC-GUI: a Shiny-based application for differential expression analysis of RNA-Seq count data. *BMC research notes* **12:**133.

Takayama K, Morisaki Y, Kuno S, Nagamoto Y, Harada K, Furukawa N, Ohtaka M, Nishimura K, Imagawa K, and Sakurai F (2014) Prediction of interindividual differences in hepatic functions and drug sensitivity by using human iPS-derived hepatocytes. *Proceedings of the National Academy of Sciences* **111:**16772-16777.

Takayama K, Negoro R, Yamashita T, Kawai K, Ichikawa M, Mori T, Nakatsu N, Harada K, Ito S, and Yamada H (2019) Generation of Human iPSC–Derived Intestinal Epithelial Cell Monolayers by CDX2 Transduction. *Cellular and molecular gastroenterology and hepatology* **8:**513-526.

Taketani M, Shii M, Ohura K, Ninomiya S, and Imai T (2007) Carboxylesterase in the liver and small intestine of experimental animals and human. *Life sciences* **81:**924-932.

Teubner W, Meinl W, Florian S, Kretzschmar M, and Glatt H (2007) Identification and localization of soluble sulfotransferases in the human gastrointestinal tract. *Biochemical Journal* **404:**207-215.

Theodoropoulos C, Demers C, Delvin E, Ménard D, and Gascon - Barré M (2003) Calcitriol regulates the expression of the genes encoding the three key vitamin D3 hydroxylases and the drug - metabolizing enzyme CYP3A4 in the human fetal intestine. *Clinical endocrinology* **58:**489-499.

Vaessen SF, van Lipzig MM, Pieters RH, Krul CA, Wortelboer HM, and van de Steeg E (2017) Regional expression levels of drug transporters and metabolizing enzymes along the pig and human intestinal tract and comparison with Caco-2 cells. *Drug Metabolism and Disposition* **45:**353-360.

van de Kerkhof EG, de Graaf IA, Ungell A-LB, and Groothuis GM (2008) Induction of metabolism and transport in human intestine: validation of precision-cut slices as a tool to study induction of drug metabolism in human intestine in vitro. *Drug*

Metabolism and Disposition **36:**604-613.

von Richter O, Greiner B, Fromm MF, Fraser R, Omari T, Barclay ML, Dent J, Somogyi AA, and Eichelbaum M (2001) Determination of in vivo absorption, metabolism, and transport of drugs by the human intestinal wall and liver with a novel perfusion technique. *Clinical Pharmacology & Therapeutics* **70:**217-227.

Wagner GP, Kin K, and Lynch VJ (2012) Measurement of mRNA abundance using RNA-seq data: RPKM measure is inconsistent among samples. *Theory in biosciences* **131:**281-285.

Wingett SW and Andrews S (2018) FastQ Screen: A tool for multi-genome mapping and quality control. *F1000Research* **7**.

Zhang H, Wolford C, Basit A, Li AP, Fan PW, Murray BP, Takahashi RH, Khojasteh SC, Smith BJ, and Thummel KE (2020) Regional proteomic quantification of clinically relevant non-cytochrome P450 enzymes along the human small intestine. *Drug Metabolism and Disposition* **48:**528-536.

Zhang Q-Y, Dunbar D, Ostrowska A, Zeisloft S, Yang J, and Kaminsky LS (1999) Characterization of human small intestinal cytochromes P-450. *Drug Metabolism and Disposition* **27:**804-809.

DMD Fast Forward. Published on December 31, 2020 as DOI: 10.1124/dmd.120.000283
This article has not been copyedited and formatted. The final version may differ from this version.

Footnotes

Disclosure statement

No author has an actual or perceived conflict of interest with the contents of this article.

Financial support

Funding: This research is supported by the grants from JSPS KAKENHI Grant Number (18H05033, 18H05373).

The name and full address and e-mail address of person to receive reprint requests.

Dr. Hiroyuki Mizuguchi

Laboratory of Biochemistry and Molecular Biology, Graduate School of Pharmaceutical Sciences, Osaka University, 1-6 Yamadaoka, Suita, Osaka 565-0871, Japan.

Phone: +81-6-6879-8185, FAX: +81-6-6879-8187

E-mail: mizuguch@phs.osaka-u.ac.jp

DMD Fast Forward. Published on December 31, 2020 as DOI: 10.1124/dmd.120.000283
This article has not been copyedited and formatted. The final version may differ from this version.

Figure Legends

Figure 1 Acquisition of intestinal biopsy samples

(**A**) An image of the inside of the duodenum was taken using an endoscopic camera. (**B**) The duodenal epithelial layer was collected using forceps. (**C**) Three pieces of an intestinal biopsy sample were collected. (**D**) Acquisition regions and the numbers of patients providing intestinal biopsy samples from each. (**E**) Patient information (gender and race) for each intestinal biopsy sample. Some samples were obtained from patients treated with prednisolone or budesonide. Samples exposed to prednisolone or budesonide are marked with a *1 or *2, respectively. Note that 14 patients participated in this analysis and 23 samples were acquired. The analysis thus included cases in which samples from multiple sites were collected from the same patient. RIN: RNA Integrity Number.

Figure 2 Global gene expression analysis of intestinal biopsy samples

(**A**) The hierarchical clustering and heatmap are shown for each biopsy sample. (**B**) 2D and 3D principal component analysis (PCA) of transcription profiles was performed on biopsy samples. PC1, principal component 1; PC2, principal component 2; PC3, (principal component 3). The ratio of the contribution of each component is shown. Duodenum, yellow; rectum, gray; ileum, blue; colon, red.

Figure 3 Expression analysis of CYPs in various regions of the intestinal tract

(**A**) The expression profiles of *CYPs* in the ileum are shown. (**B**) The gene expression levels of *CYP3A4*, *CYP2C19*, *CYP3A5*, and *CYP2C18* in the duodenum, ileum, colon,

and rectum are examined.

Figure 4　Expression analysis of non-CYP enzymes in various regions of the intestinal tract

(**A**) The expression profiles of non-CYP enzymes in the ileum are shown. (**B**) The gene expression levels of *CES2*, *MAOA*, *DPYD*, and *AKR1B10* in the duodenum, ileum, colon, and rectum are examined.

Figure 5　Expression analysis of intestinal transporters in various regions of the intestinal tract

(**A**) The expression profiles of intestinal transporters in the ileum are shown. (left: apical transporters, right: basolateral transporters) (**B**) The gene expression levels of *ASBT*, *P-gp*, *BCRP*, and *PEPT1* in the duodenum, ileum, colon, and rectum are examined.

Figure 6　Expression analysis of nuclear receptors in various regions of the intestinal tract

(**A**) The expression profiles of nuclear receptors in the ileum are shown. (**B**) The gene expression levels of *FXR*, *VDR*, *GR*, and *PXR* in the duodenum, ileum, colon, and rectum are examined.

Figure 7　Expression analysis of UGTs in various regions of the intestinal tract

(**A**) The expression profiles of *UGTs* in the ileum are shown. (**B**) The gene expression levels of *UGT2A3*, *UGT1A8*, *UGT1A1*, and *UGT2B7* in the duodenum, ileum, colon, and rectum are examined.

DMD Fast Forward. Published on December 31, 2020 as DOI: 10.1124/dmd.120.000283
This article has not been copyedited and formatted. The final version may differ from this version.

Figure 8　Expression analysis of carboxylesterases and SULTs in various regions of the intestinal tract

(**A**) The expression profiles of carboxylesterases and *SULTs* in the ileum are shown. (**B**) The gene expression levels of *SULT1A4*, *SULT1A3*, *SULT1A1*, and *SULT1B1* in the duodenum, ileum, colon, and rectum are examined.

Figure 9　Duodenum-, ileum-, colon-, and rectum-specific markers

Duodenum-, ileum-, colon-, and rectum-specific markers are shown in this figure.

Figure 10　Global gene expression analysis of human iPS cell-derived intestinal epithelial cells and Caco-2 cells

Principal component analysis of transcription profiles was performed on biopsy samples, human iPS cell-derived intestinal epithelial cells cultured in general cell culture dishes (human iPS-ELC (flat)), human iPS cell-derived intestinal epithelial cells cultured on cell culture inserts (human iPS-ELC (monolayer)), and Caco-2 cells. PC1, principal component 1; PC2, principal component 2; PC3, principal component 3. The ratio of the contribution of each component is shown.

Figure 1

A

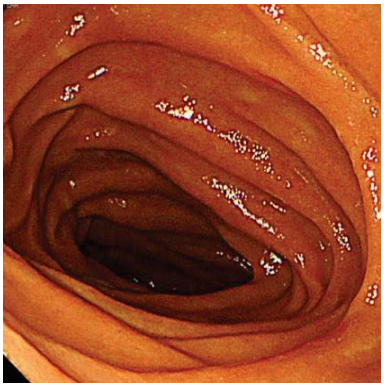

B

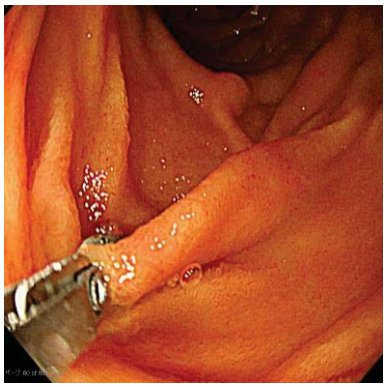

C

D

segment	number of patient
Duodenum	4
Jejunum	0
Ileum	7
Colon	10
Rectum	2
total	23

E

Region	RIN	Sex	Age	Race
Colon	7.4	male	33	Japanese
Colon	7.3	male	22	Japanese
Colon	7.2	male	22	Japanese
Colon	7.8	male	40	Japanese
Colon*1	8.6	male	54	Japanese
Colon	7.9	male	51	Japanese
Colon	8.1	male	27	Japanese
Colon	8.4	male	44	Japanese
Colon	8.9	male	23	Japanese
Colon	7.1	female	29	Japanese
Duodenum	8	male	53	Japanese
Duodenum*2	7.4	male	42	Japanese
Duodenum*2	8.4	male	54	Japanese
Duodenum	8.3	male	51	Japanese
Ileum	7.4	male	33	Japanese
Ileum	8	male	54	Japanese
Ileum*1	8.7	male	54	Japanese
Ileum	7.8	male	51	Japanese
Ileum	7.8	male	44	Japanese
Ileum	8.7	male	23	Japanese
Ileum	8.5	female	29	Japanese
Rectum	8.8	male	54	Japanese
Rectum	8.2	male	51	Japanese

Figure 2

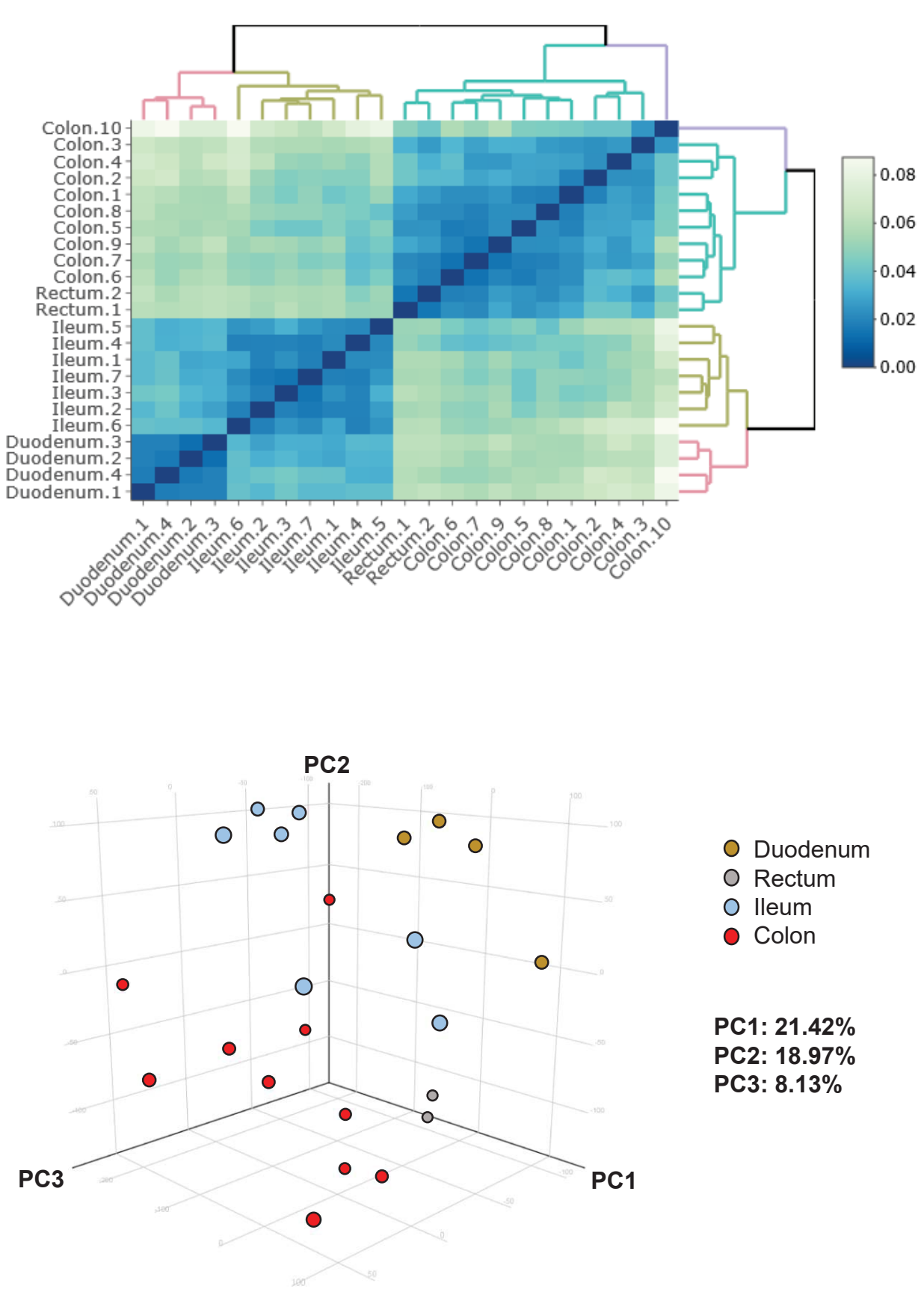

Figure 3

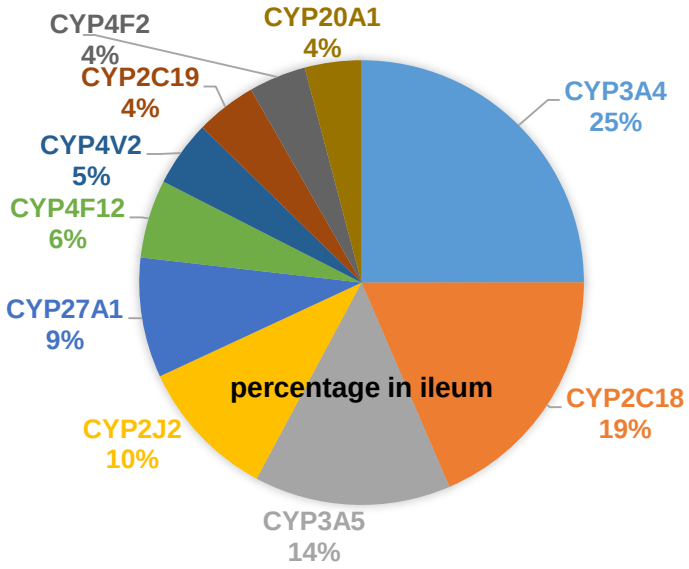
CYP4F2
4%
CYP20A1
4%
CYP2C19
4%
CYP3A4
25%
CYP4V2
5%
CYP4F12
6%
CYP27A1
9%
percentage in ileum
CYP2C18
19%
CYP2J2
10%
CYP3A5
14%

B

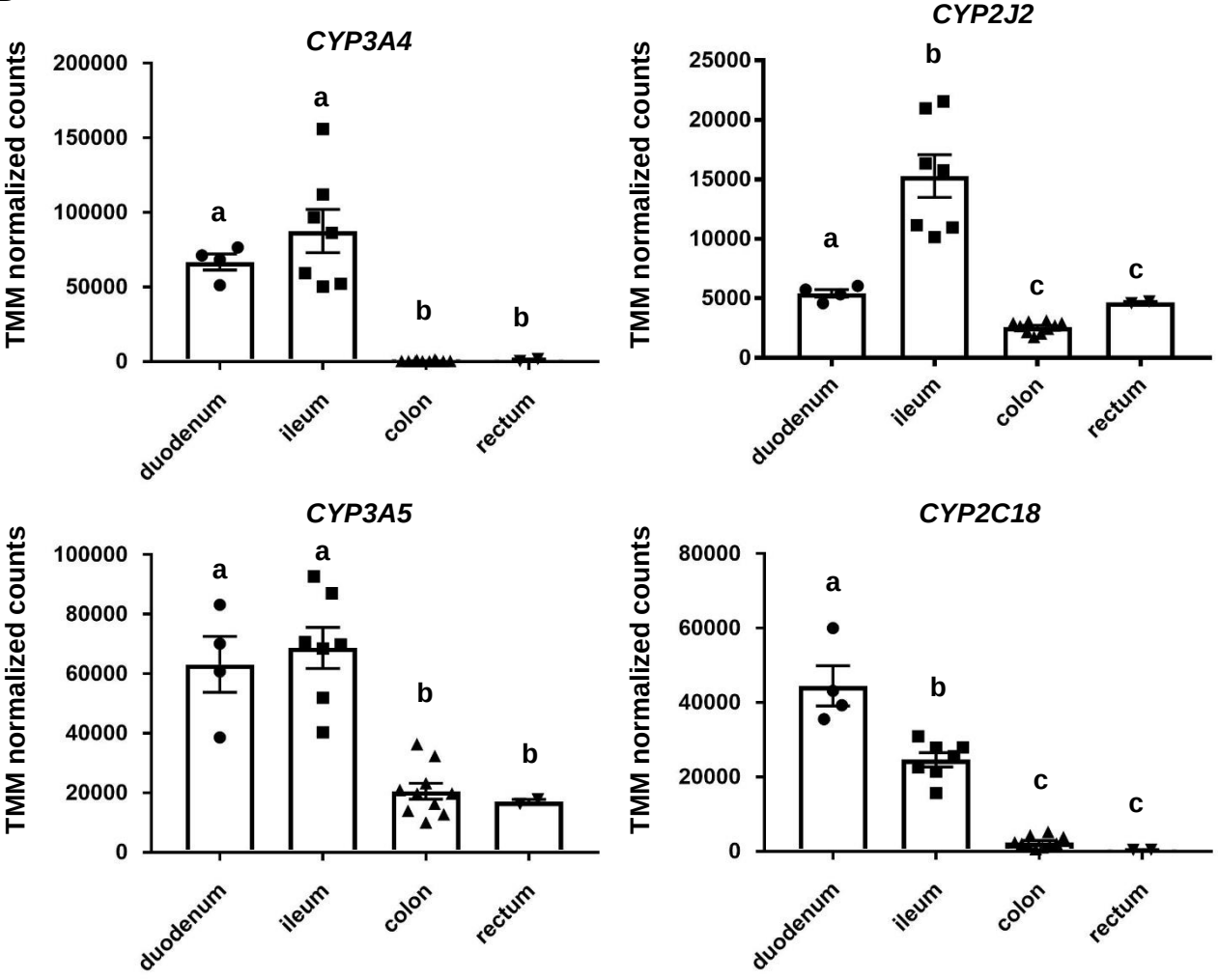
CYP3A4
TMM normalized counts
200000
150000
100000
50000
0
a
a
b
b
duodenum
ileum
colon
rectum
CYP2J2
TMM normalized counts
25000
20000
15000
10000
5000
0
a
b
c
c
duodenum
ileum
colon
rectum
CYP3A5
TMM normalized counts
100000
80000
60000
40000
20000
0
a
a
b
b
duodenum
ileum
colon
rectum
CYP2C18
TMM normalized counts
80000
60000
40000
20000
0
a
b
c
c
duodenum
ileum
colon
rectum

Figure 4

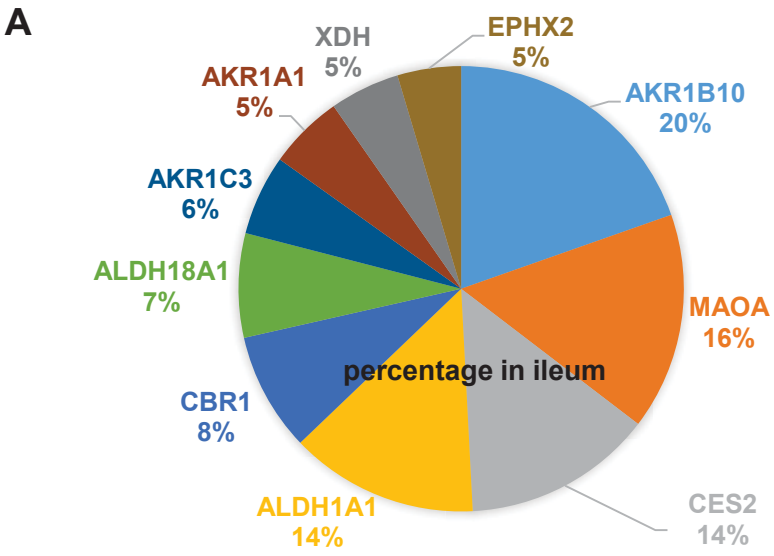

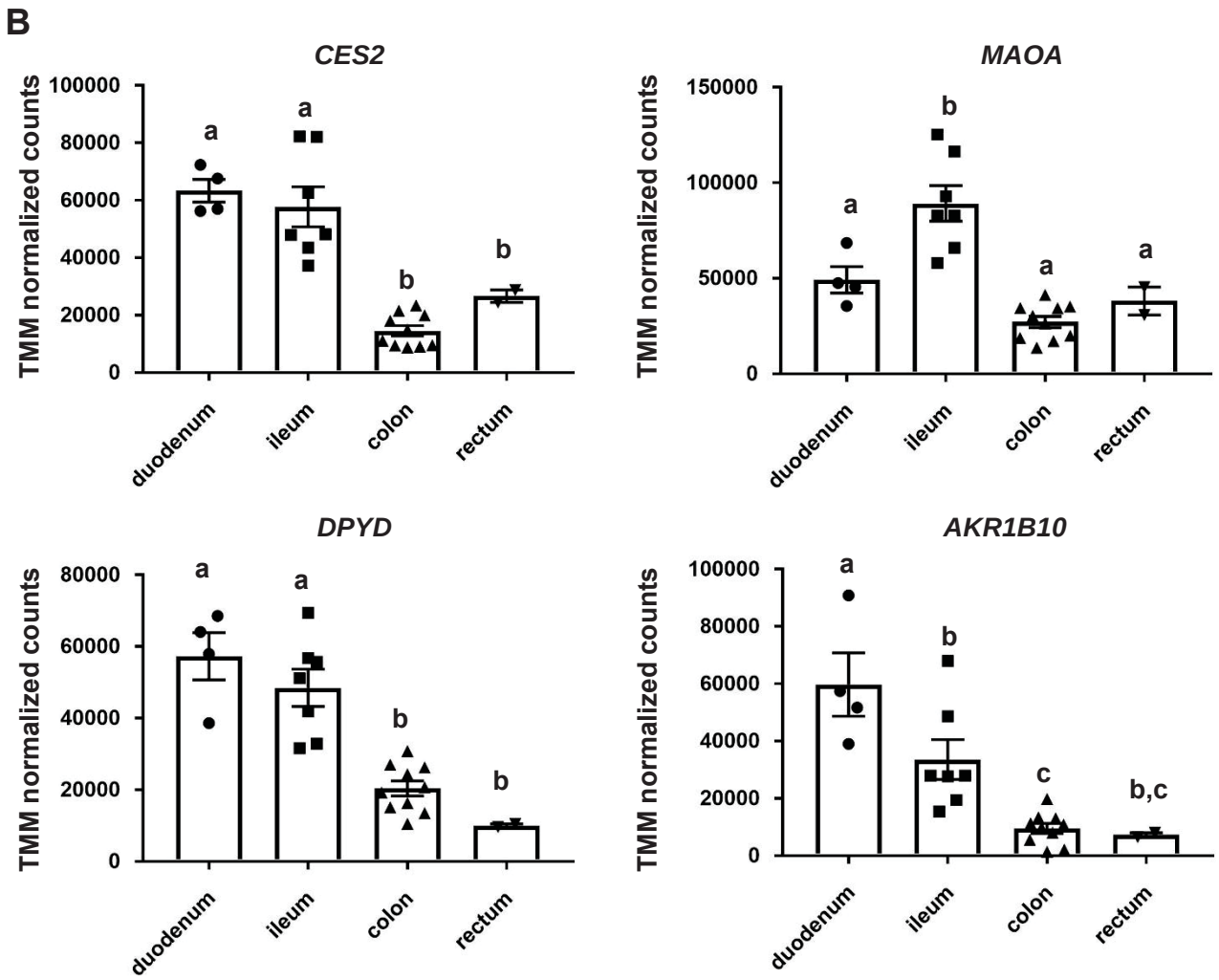

Figure 5

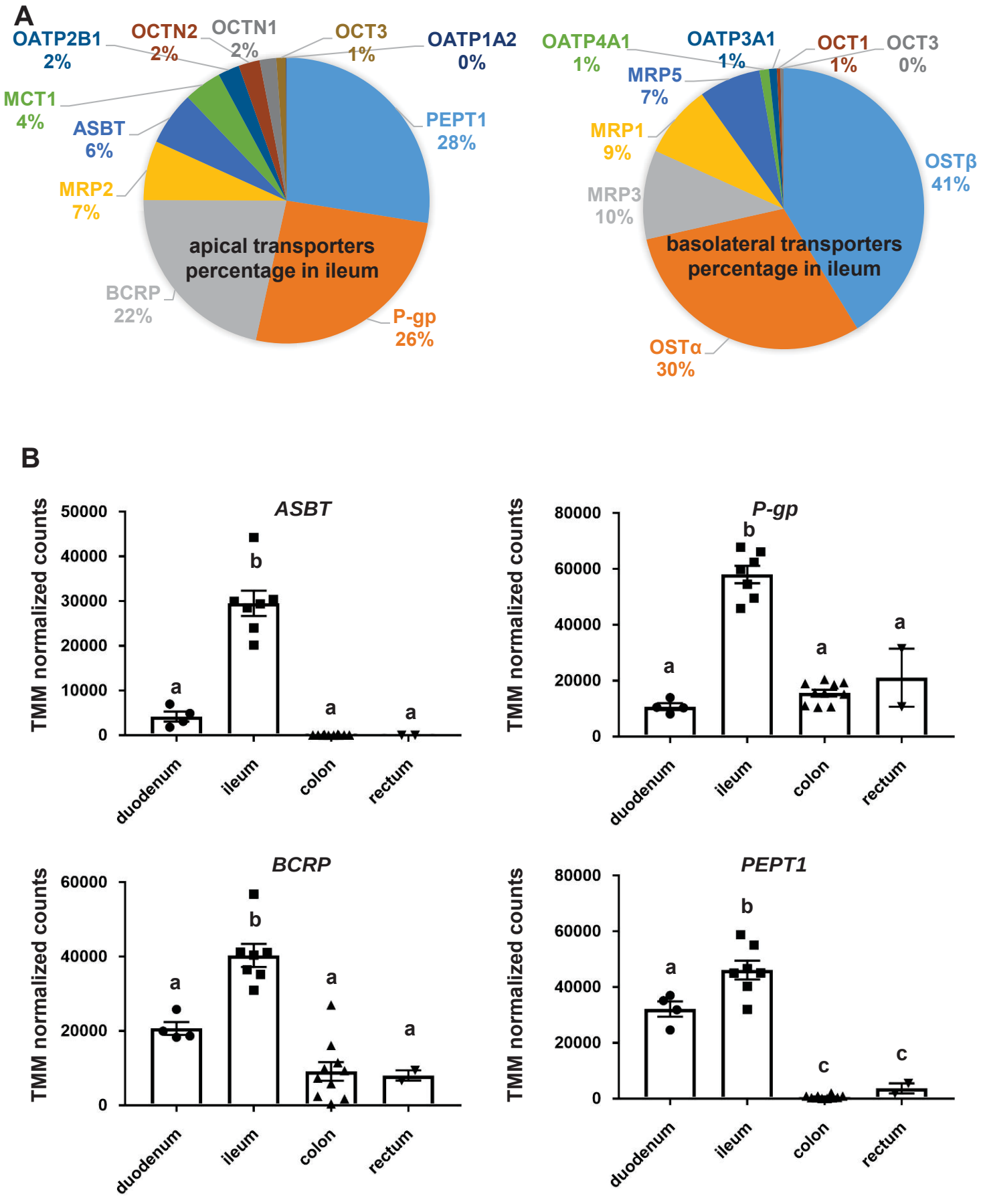

Figure 6

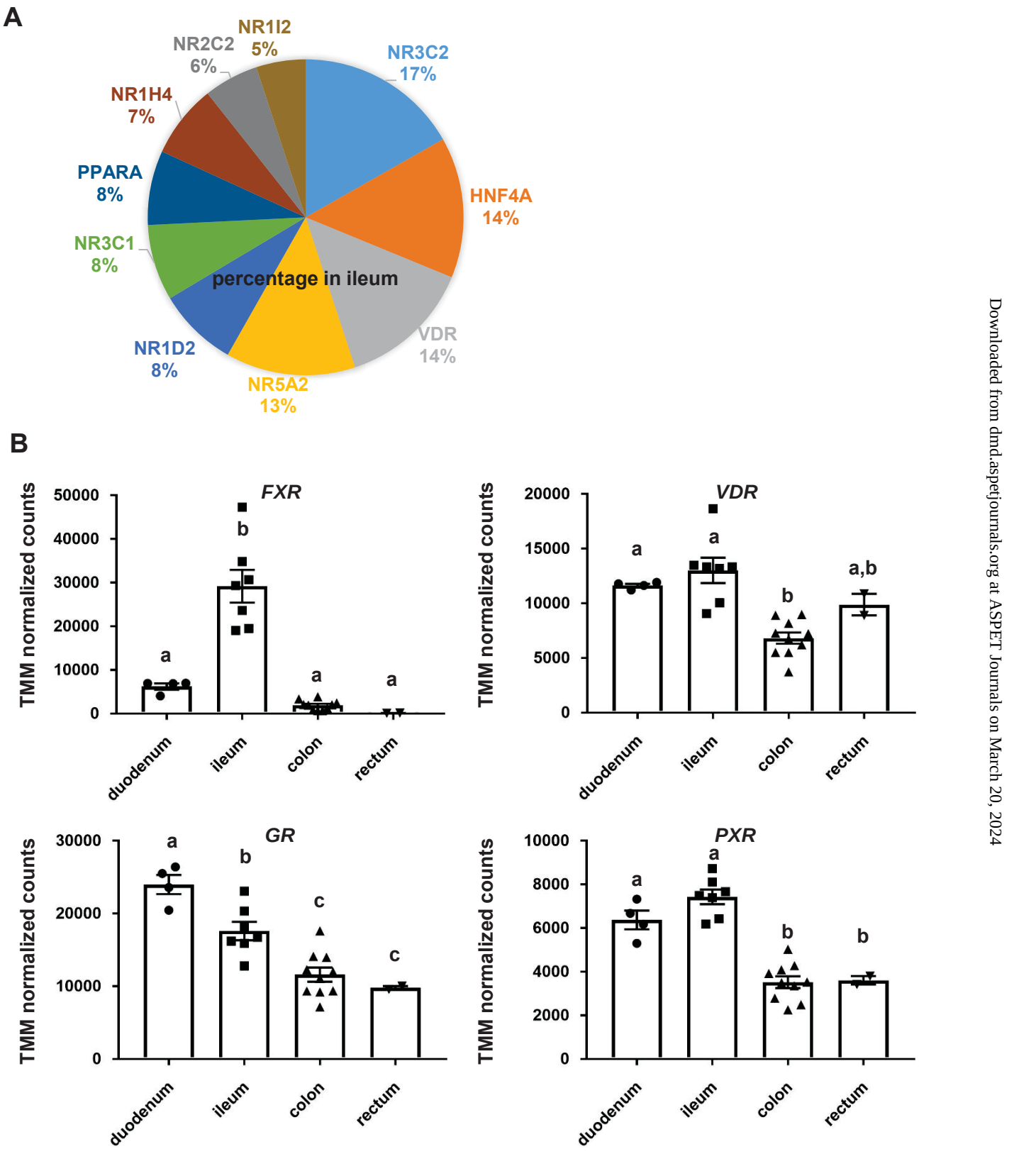

Figure 7

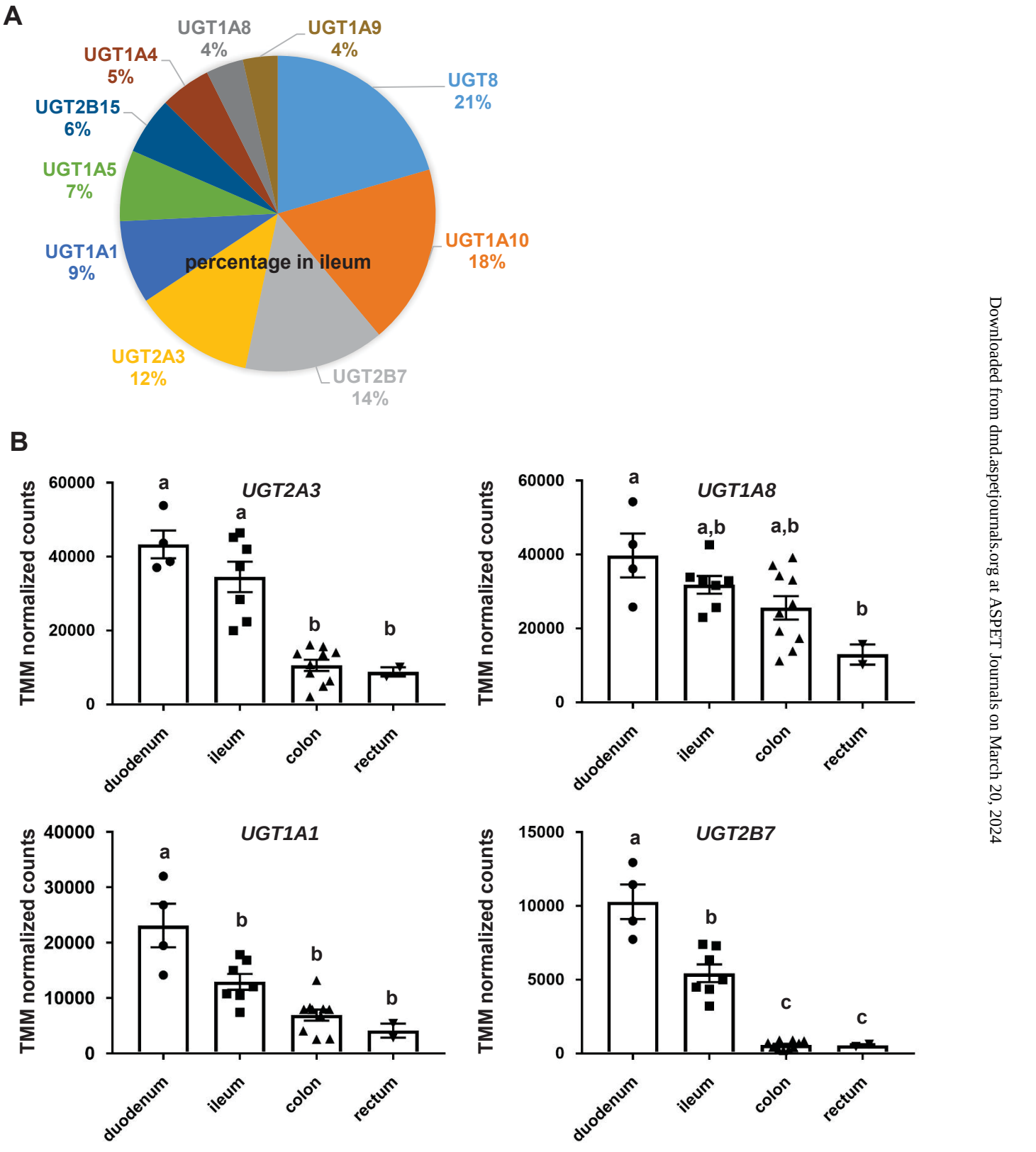

Figure 8

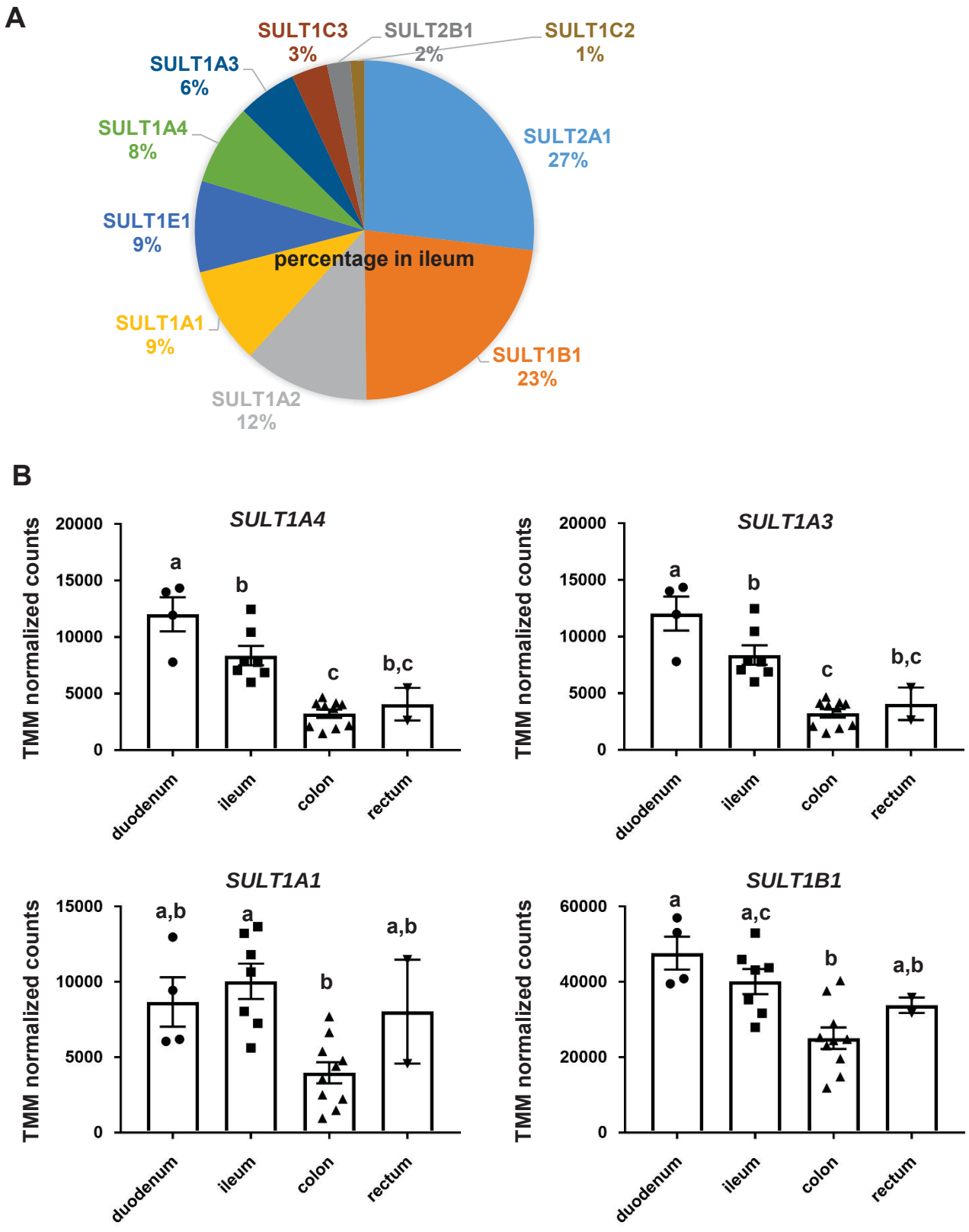
A
SULT1C3
3%
SULT2B1
2%
SULT1C2
1%
SULT1A3
6%
SULT1A4
8%
SULT2A1
27%
SULT1E1
9%
percentage in ileum
SULT1A1
9%
SULT1B1
23%
SULT1A2
12%
B
SULT1A4
SULT1A3
SULT1A1
SULT1B1
TMM normalized counts
duodenum
ileum
colon
rectum
a
b
c
b,c
a,b
a,c

Figure 9

region specific markers

	duodenum	ileum	colon	rectum
TMPRSS15	**505225.76**	9003.13	63.23	49.71
FOLH1	**53713.26**	368.78	58.37	34.91
ADA	**20163.06**	241.90	227.19	141.16
ONECUT2	**20026.18**	105.17	71.33	85.69
FOLH1B	**13849.37**	104.14	18.05	10.81
GATA4	**9314.30**	35.68	6.34	3.73
AQP10	**6364.43**	10.60	1.70	0.97
NPC1L1	**4710.76**	130.16	12.52	6.12
MLN	**3369.15**	11.40	2.94	3.88
CCK	**3300.35**	42.44	2.88	0.97
AF015720.1	**2015.27**	26.43	10.22	2.98
SULT4A1	**1302.64**	4.15	6.08	7.09
AC013275.1	**1281.52**	8.61	4.92	7.24
ST8SIA3	**1243.50**	8.35	2.96	3.36
AC090340.1	**1102.33**	1.20	1.20	0.97
AL354980.1	**532.89**	1.52	1.20	0.97
C8A	**262.61**	4.02	3.04	0.97
C8orf49	**117.34**	1.40	1.20	0.97
SLC5A12	5322.49	**45978.79**	92.38	196.49
NTS	345.94	**22227.00**	62.10	3.05
CPO	120.55	**20357.30**	50.75	37.91
HOXC6	8.86	**280.39**	20.25	6.93
CD177	4.05	72.76	**16808.29**	812.30
AC005392.3	4.15	54.02	**12214.74**	604.53
CD177P1	1.14	16.61	**3928.35**	184.37
L1TD1	25.88	54.34	**1818.60**	296.40
PWRN1	46.99	48.61	**1011.04**	199.11
RF00019	1.14	1.52	**20.03**	0.97
CLDN8	2.25	501.96	1226.55	**9350.77**
HOXB13	1.73	4.35	697.47	**9140.55**
GLDN	121.53	87.45	1150.41	**6320.24**
ST6GAL2	31.26	17.42	1123.54	**6147.36**
HOXD10	1.14	2.17	192.41	**3716.11**
PRAC1	1.14	2.26	445.26	**2199.63**
HOXD13	1.14	1.32	7.96	**1893.20**
AC108865.1	7.91	4.76	49.11	**997.00**
HOXD11	1.14	1.20	41.55	**932.06**
RBM24	30.33	31.42	104.19	**764.09**
AC108865.2	2.22	1.78	9.43	**271.92**
TNNC1	6.08	6.16	12.65	**252.31**
EVX2	1.14	1.20	1.27	**235.16**
HOXD12	1.14	1.20	1.20	**194.76**
AC091179.1	1.14	1.20	4.02	**48.04**
LINC01445	1.63	1.40	2.69	**39.42**

Figure 10